Annals of Anatomy 249 (2023) 152104

Contents lists available at ScienceDirect

Annals of Anatomy

journal homepage: www.elsevier.com/locate/aanat

RESEARCH ARTICLE

SHRSP5/Dmcr rats fed a high-fat and high-cholesterol diet develop disease-induced sarcopenia as nonalcoholic steatohepatitis progresses

Shusei Yamamoto [a,b], Koki Honma [b], Moe Fujii [c], Mai Kakimoto [b], Sora Kirihara [b], Hinako Nakayama [b], Kazuya Kitamori [d], Ikumi Sato [a,b], Satoshi Hirohata [a], Shogo Watanabe [a,*]

[a] Faculty of Health Sciences, Okayama University, 2-5-1, Shikata-cho, Kita-ku, Okayama-shi, Okayama 700-8558, Japan
[b] Department of Medical Laboratory Science, Graduate School of Health Sciences, Okayama University, 2-5-1, Shikata-cho, Kita-ku, Okayama-shi, Okayama 700-8558, Japan
[c] Department of Medical Technology, Ehime Prefectural University of Health Sciences, 543, Takoda, Tobe-cho, Iyo-gun, Ehime 791-2101, Japan
[d] College of Human Life and Environment, Kinjo Gakuin University, 2-1723, Omori, Moriyama-ku, Nagoya-shi, Aichi 463-8521, Japan

ARTICLE INFO

Article history:
Received 4 January 2023
Received in revised form 7 March 2023
Accepted 10 May 2023
Available online 18 May 2023

Keywords:
Sarcopenia
Nonalcoholic steatohepatitis
SHRSP5/Dmcr
High-fat and high-cholesterol diets

ABSTRACT

Background: Secondary sarcopenia develops as a result of a bedridden state and illnesses, such as cachexia, liver disease, and diabetes. However, there is a lack of animal models to investigate the underlying mechanisms and potential treatments for secondary sarcopenia. Recently, secondary sarcopenia has been associated with the prognosis of nonalcoholic steatohepatitis. This study aimed to investigate whether stroke-prone spontaneously hypertensive rat 5 (SHRSP5/Dmcr) which developed severe nonalcoholic steatohepatitis by a high-fat and high-cholesterol (HFC; containing 2% cholic acid) diet is a useful model of secondary sarcopenia.

Methods: SHRSP5/Dmcr rats were divided into 6 groups fed with a Stroke-Prone (SP: normal chow) or HFC diets for different periods (4, 12, and 20 weeks), and WKY/Izm rats were divided into 2 groups fed an SP or HFC diet. Body weight, food intake, and muscle force were measured weekly for all rats. After the end of the diet period, skeletal muscle strength evoked by electrical stimulation was recorded, blood was collected, and organ weight was measured. The sera were used for biochemical analysis and the organs were used for histopathological analysis.

Results: SHRSP5/Dmcr rats fed an HFC diet developed nonalcoholic steatohepatitis, and their skeletal muscles, especially fast muscles, showed atrophy, indicating that muscle atrophy is aggravated by the progression of nonalcoholic steatohepatitis. In contrast, WKY/Izm rats fed an HFC diet did not exhibit sarcopenia.

Conclusions: This study suggests that SHRSP5/Dmcr rats could be a useful novel model for investigate the mechanism of secondary sarcopenia disorder associated with nonalcoholic steatohepatitis.

1. Introduction

Sarcopenia is a disease characterized by skeletal muscle mass loss. Sarcopenia was initially thought to be an age-related disease; however, sarcopenia induced by age is now defined as primary sarcopenia whereas sarcopenia caused by malnutrition and diseases, including cachexia, diabetes, chronic kidney disease, is defined as secondary sarcopenia (Liccini and Malmstrom, 2016; Meza-Valderrama et al., 2021; Sabatino et al., 2021). In addition to skeletal muscle mass loss, sarcopenia is characterized by a decrease in muscle strength and/or physical function (Chen et al., 2020; Cruz-Jentoft and Sayer, 2019). Moreover, the prognosis of sarcopenia is worse in patients with malnutrition and other diseases. As older adults are more likely to develop sarcopenia, early therapeutic diagnosis and intervention are key to the treatment of sarcopenia, especially in developed countries with aging populations. Treatments for sarcopenia include exercise and branched-chain amino acid replacement therapy; however, the therapeutic effects of these

Abbreviations: ALB, albumin; ALT, alanine transaminase; AST, aspartate transaminase; A/G, albumin/globulin; EDL, extensor digitorum longus muscle; HE, hematoxylin and eosin; HFC, high-fat and high-cholesterol; IHC, immunohistochemical; NAFL, nonalcoholic fatty liver; NAFLD, nonalcoholic fatty liver disease; NAS, nonalcoholic fatty liver disease activity score; NASH, nonalcoholic steatohepatitis; SHRSP5, stroke-prone spontaneously hypertensive rat 5; SOL, soleus muscle; SP, stroke-prone; T-Chol, total cholesterol; TG, triglyceride; WKY, Wister Kyoto

* Corresponding author.
E-mail address: watanabe1224@okayama-u.ac.jp (S. Watanabe).

https://doi.org/10.1016/j.aanat.2023.152104
0940-9602/

treatments are not clear (Hiraoka et al., 2017; Mohta et al., 2022). Therefore, basic research is needed to validate prevention and/or treatment methods for sarcopenia.

Nonalcoholic fatty liver disease (NAFLD) is a phenotype of metabolic syndrome. NAFLD is classified into 2 phenotypes: nonalcoholic fatty liver (NAFL), which is characterized by a fatty liver, and nonalcoholic steatohepatitis (NASH), which is characterized by steatosis and fibrosis. In recent years, approximately 25–45% of the world's population has been affected by NAFLD, and 20% of patients with NAFL progress to NASH (Nd, 2019; Rinella, 2015). Moreover, some patients with NAFLD/NASH develop cirrhosis and hepatocellular carcinoma (Younossi et al., 2016). The relationship between NAFLD/NASH and sarcopenia has received significant attention in recent years; sarcopenia is associated with a poor prognosis in patients with NAFLD/NASH (Habig et al., 2021; Koo et al., 2017; Lee et al., 2015; Yu et al., 2018). Sarcopenia has been implicated in the pathogenesis of NAFLD/NASH independently of aging, obesity, and insulin resistance, and in lean NASH, which is particularly problematic in Asian countries (Koo et al., 2017; Younes and Bugianesi, 2019). In addition, protein-energy malnutrition and hyperammonemia were reported to be associated with sarcopenia and chronic liver diseases, including NAFLD/NASH. Although animal models of NAFLD/NASH with sarcopenia for basic research have been reported, these animals exhibited mild hepatic fibrosis whereas severe hepatic fibrosis has been observed as the pathological manifestation of sarcopenia in humans. Therefore, an optimal animal model of sarcopenia has not been established yet (Cabrera et al., 2016; Nachit et al., 2021).

Stroke-prone spontaneously hypertensive rat 5 (SHRPS5/Dmcr) is an animal that develops NASH with severe fibrosis when fed a high-fat and high-cholesterol (HFC) diet (Kitamori et al., 2012). In this study, we investigated the physiological, biochemical, and pathological changes in SHRSP5/Dmcr rats fed an HFC diet for 4, 12, and 20 weeks, and investigated its use as a new animal model for disease-induced sarcopenia.

2. Material and methods

2.1. Animal models and diets

All animal experiments were performed in strict accordance with the recommendations of the standards of Care and Management of Laboratory Animals and Relief of Pain published by the Japanese Ministry of Environment (2006). In this study, all rats were maintained in a temperature- (24 °C ± 2 °C) and humidity-controlled (55% ± 5%) facility with a 12-hour light/dark cycle. This study was approved by the Animal Experiment Committee of Okayama University (approval No. OKU-2021208).

Nine-week-old male SHRSP5/Dmcr (n = 30) and WKY/Izm (n = 10) rats were provided by the Disease Model Cooperative Research Association (Kyoto, Japan). SHRSP5/Dmcr rats were established using outbred WKY/Izm rats (Kozaki et al., 2015; Sweet et al., 2015). SP (20.8% crude protein, 4.8% crude lipid, 3.2% crude fiber, 5.0% crude ash, 8.0% moisture, and 58.2% carbohydrate) and HFC diets (9.6% crude protein, 24.0% crude lipid, 1.5% crude fiber, 2.3% crude ash, 3.7% moisture, 26.9% carbohydrate, 25.0% palm oil, 5.0% cholesterol, and 2.0% cholic acid) were obtained from Funabashi Farm (Chiba, Japan) (Kitamori et al., 2012). The rats consumed water and SP diet (control chow) ad libitum to acclimatize to the location in the first week. At 10 weeks of age, the SHRSP5/Dmcr rats were divided into 6 groups, and the WKY/Izm rats were divided into 2 groups as fellows (Fig. 1A): (i) SHRSP5/Dmcr + SP diet for 4 weeks (S4 group, n = 5), (ii) SHRSP5/Dmcr + HFC diet for 4 weeks (H4 group, n = 5), (iii) SHRSP5/Dmcr + SP diet for 12 weeks (S12 group, n = 5), (iv) SHRSP5/Dmcr + HFC diet for 12 weeks (H12 group, n = 5), (v) SHRSP5/Dmcr + SP diet for 20 weeks (S20 group, n = 5), (vi) SHRSP5/Dmcr + HFC diet for 20 weeks (H20 group, n = 5), (vii) WKY/Izm + SP diet for 20 weeks (S20W group, n = 5), and (viii) WKY/Izm + HFC diet for 20 weeks (H20W group, n = 5). Body weight and food intake were measured weekly.

2.2. Measurement of muscle strength

Extremity limb grip strength was measured using a spring scale (range: 2 kg, resolution: 20 g) and recorded using a camera. The wire mesh was connected to a spring scale, the rat grabbed the wire mesh, and its tail was pulled until the rat released the wire mesh. The spring scale was recorded through videos using a camera, and the maximum value was recorded when the rat released the wire mesh (Supplementary Fig. 1). Measurements were performed 4–5 times, and the average of the 3 highest values was used for validation. An interval of approximately 10 min was allowed between each measurement.

Muscle strength evoked by electrical stimulation was recorded in the extensor digitorum longus muscle (EDL) and soleus muscle (SOL) using MP100 and AcqKnowledge (BIOPAC Systems, Inc., Goleta, CA, USA). The rats were anesthetized with pentobarbital sodium salt (Nacalai Tesque, Inc., Kyoto, Japan) dissolved in distilled water at a concentration of 64.8 mg/mL and administered intraperitoneally at a dose of 48.6 mg/kg. Each rat was placed on a stand in a face-down position, and a skin incision was made on the left leg with shaved body hair to detach the gastrocnemius muscle and expose the SOL. The tendon on the terminal side was dissected and immediately hooked to a transducer (TSD125D; BIOPAC Systems) connected to a general-purpose amplifier (DA100C; BIOPAC Systems) and subjected to a constant tension load (3 g force). A stimulating electrode (UM2–5050; Unique Medical Co., Ltd., Tokyo, Japan) was hooked to the dominant nerve and stimulated at 5 V/1000 ms (square wave pulse) at an interval of 2 s using an electrical stimulator (STM100C; BIOPAC Systems) and isolator (STMISOC; BIOPAC Systems). The contraction force was recorded 10 times (sampling frequency was 2000 Hz), and the median of 3 data points was averaged. After SOL strength measurements, each rat was placed on a stand in a face-up position, a skin incision was made to detach the tibialis anterior muscle, exposing the EDL, and contractility was measured as described for SOL (Supplementary Fig. 2). The contraction force was converted from voltage (V) to g force (gf).

2.3. Dissection and biochemical analysis

At 14, 22, and 30 weeks of age, we obtained blood samples from the right carotid artery of rats, which were fasted overnight, under anesthesia after measurement of muscle strength. The sample was then centrifuged at 2500 rpm for 20 min, and the serum was collected and stored at −80 °C until analysis. Aspartate aminotransferase (AST), alanine aminotransferase (ALT), albumin (ALB), globulin, ALB/globulin (A/G) ratio, total cholesterol (T-Chol), and triglyceride (TG) levels were measured using routine laboratory methods (Oriental Yeast Co. Ltd., Tokyo, Japan). After blood sampling and refluxing in phosphate-buffered saline (Kanto Chemical Co., Inc., Tokyo, Japan), the liver, spleen, EDL, and SOL were obtained, weighted, and sectioned for histopathological analysis, except the spleen.

2.4. Histopathological analysis

The liver, EDL, and SOL were fixed in 10% formalin (KENEI Pharmaceutical Co., Ltd., Osaka, Japan) for 48 h, embedded in paraffin, and sectioned for histological analysis. Vertical (liver) and transverse (EDL and SOL) Section (4 μm) were stained with hematoxylin and eosin (HE) staining, and livers were stained with Masson-trichrome staining for NAFLD activity score (NAS) and Ishak

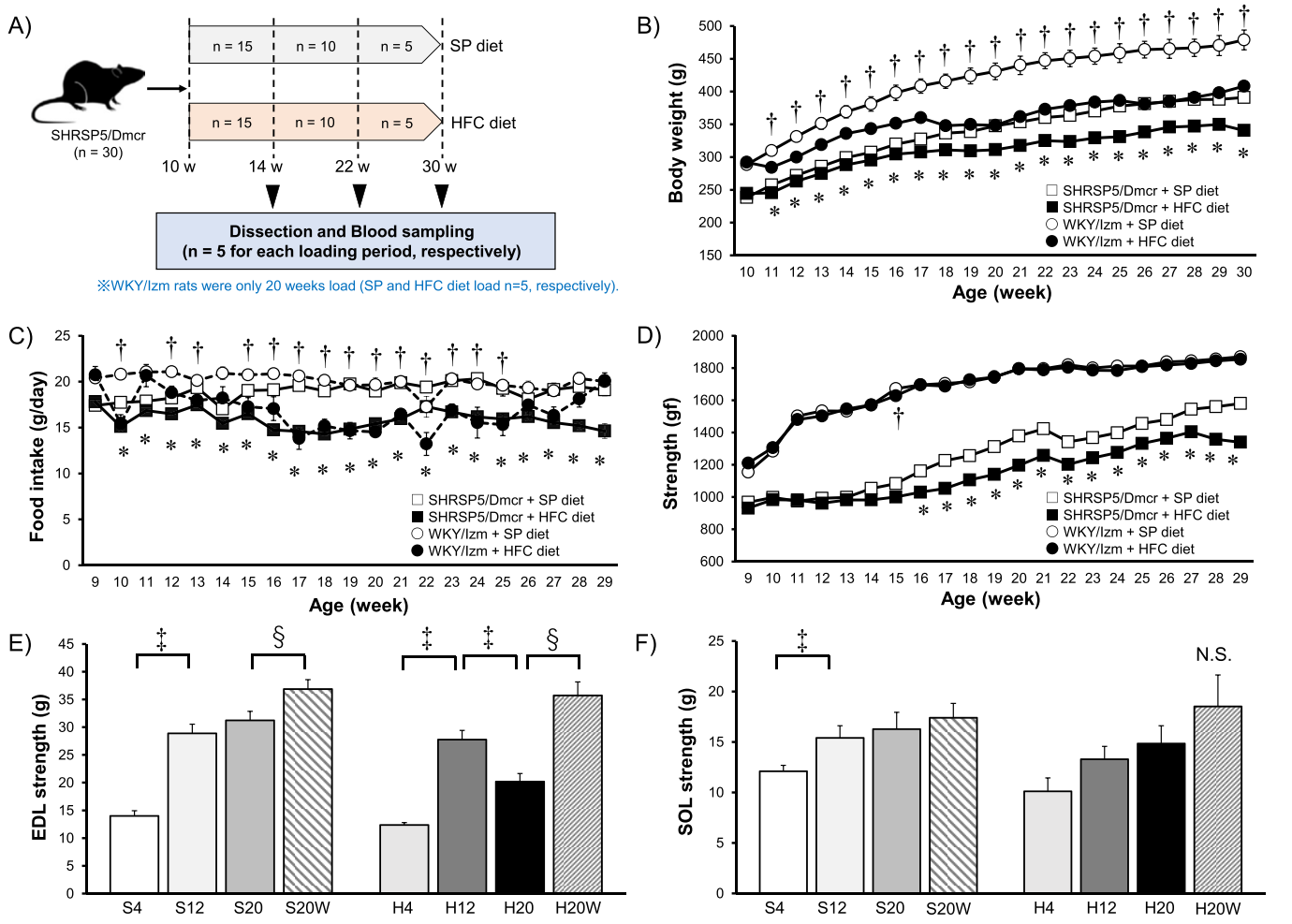

Fig. 1. Schematic illustration of the experimental design and physiological data. (A) Ten-week-old SHRSP5/Dmcr rats were divided into the SP and HFC groups (n = 15, each). An autopsy was performed at 14 (S4 and H4 groups, n = 5 per group), 22 (S12 and H12 groups, n = 5 per group), and 30 weeks of age (S20 and H20 groups, n = 5 per group). WKY/Izm rats were fed either diet for 20 weeks (S20W and H20W groups, n = 5 per group). (B, C) Body weight and food intake of the SP and HFC groups. Both body weight and food intake were a trend of low levels in the HFC groups compared to the SP groups. (D) Limb muscle strength in the SP and HFC groups. The HFC groups of SHRSP5/Dmcr rats were lower than the SP groups after 16 weeks of age and trended to decrease at 28 weeks of age. (E, F) The electrically evoked muscle strength of EDL and SOL in the SP and HFC groups. EDL in the H20 group was decreased. All data are mean ± standard error. * ; Significant differences were observed between SHRSP5/Dmcr rats fed SP and HFC diets for the same period, $p < 0.05$. †; Significant differences were observed between WKY/Izm rats fed SP and HFC diets for the same period, $p < 0.05$. ‡; Significant difference from SHRSP5/Dmcr rats fed the respective diet (the previous vs. following), $p < 0.05$. §; Significant difference from SHRSP5/Dmcr and WKY/Izm rats fed the respective diet for 20 weeks, $p < 0.05$. SHRSP5/Dmcr: stroke-prone spontaneously hypertensive rat 5, SP: stroke-prone, HFC: high-fat and high-cholesterol diet, WKY: Wister Kyoto, EDL: extensor digitorum longus muscle, SOL: soleus muscle.

stage. Fast muscle fibers [Myosin (FAST) clone MY-32; Sigma-Aldrich, St. Louis, MO, USA] and slow muscle fibers [Myosin (Skeletal Slow) clone NOQ7.5.4D; Sigma-Aldrich] of the S20 and H20 groups were stained using immunohistochemical (IHC) staining and the cross-sectional area of muscle fibers was measured using Image J Fiji (ImageJ 1.53 u, Java 1.8.0_322; National Institutes of Health, Bethesda, MD, USA) (Schindelin et al., 2012). The muscle fiber cross-sectional area was measured by randomly selecting one field of view (240 ×) in each specimen. All images were captured using an all-in-one fluorescence microscope (BZ-X700; Keyence, Osaka, Japan).

NAS was calculated according to the NASH Clinical Research Network scoring system that has been applied to high-fat diet-loaded rats, and ≥ 5 points were defined as NASH (Elias et al., 2009; Kleiner et al., 2005). Steatosis, inflammation, and hepatocyte ballooning were evaluated using the following classifications: (I) steatosis grades:0, none; 1, mild (5–33% of parenchymal involvement by steatosis); 2, moderate (33–66%); 3, severe (> 66%); (II) lobular inflammations:0, none; 1, mild (less than 2 foci per 200 × field); 2, moderate (2 – 4 foci per 200 × field); 3, severe (more than 4 foci per 200 × field); (III) hepatocyte ballooning:0, none; 1, few ballooning cells (less than 5 per 200 × field); and 2, many cell-prominent ballooning (more than 6 per 200 × field). According to Ishak et al. and Goodman et al., the Ishak staging system is divided into 7 stages (0 – 6) (Goodman, 2007; Ishak et al., 1995). Based on this system, the scores were defined as follows:0, none; 1, fibrous dilatation of some portal regions with or without a short fibrous septum; 2, fibrous dilatation of most portal regions with or without a short fibrous septum; 3, fibrous dilatation of most portal areas with occasional bridging from the portal-to-portal vein; 4, fibrous dilatation of most portal areas with marked bridging (both portal-to-portal and portal-to-central); 5, incomplete cirrhosis characterized by marked bridging and occasional nodules; and 6, probable or definite induration.

2.5. Statistical analysis

The relevant data are presented as mean ± standard error. Body weight, food intake, limb muscle strength, and organ weight (corrected for tibial length) were compared between SHRSP5/Dmcr and WKY/Izm rats fed different diets (SP or HFC diets). EDL and SOL strengths evoked by electrical stimulation in SHRSP5/Dmcr rats were

Table 1
The results of the biochemical analysis.

Parameters	S4	S12	S20	S20W	H4	H12	H20	H20W
AST (IU/L)	142.00 ± 17.21	90.40 ± 8.13‡	107.40 ± 5.83	116.60 ± 9.80	244.60 ± 22.55*	282.80 ± 9.02*	712.75 ± 149.26*‡	224.80 ± 8.49†§
ALT (IU/L)	54.40 ± 1.86	62.40 ± 2.48‡	60.20 ± 4.33	45.80 ± 2.20§	164.00 ± 13.81*	222.80 ± 9.99*‡	322.00 ± 33.16 *‡	142.40 ± 6.64†§
ALB (g/dL)	3.66 ± 0.10	3.78 ± 0.10	3.74 ± 0.06	4.02 ± 0.09§	4.04 ± 0.12*	3.62 ± 0.06‡	3.35 ± 0.09*‡	3.66 ± 0.09†§
Globulin (g/dL)	1.52 ± 0.04	1.78 ± 0.06‡	1.88 ± 0.07	1.98 ± 0.06	2.32 ± 0.07*	2.38 ± 0.04*	4.40 ± 1.25*‡	2.60 ± 0.09†§
A/G ratio	2.41 ± 0.05	2.14 ± 0.12	2.00 ± 0.08	2.03 ± 0.05	1.74 ± 0.02*	1.52 ± 0.02*‡	0.90 ± 0.17*‡	1.42 ± 0.07†§
T-Chol (mg/dL)	40.40 ± 1.66	60.20 ± 2.82‡	65.60 ± 2.69	149.00 ± 7.02§	89.80 ± 5.39*	165.40 ± 6.10*‡	1184.50 ± 558.03*‡	202.60 ± 12.71†§
TG (mg/dL)	18.40 ± 9.11	11.60 ± 0.93	15.60 ± 2.25	8.80 ± 1.16§	3.40 ± 0.51*	4.40 ± 0.40*	106.00 ± 68.86‡	8.20 ± 1.20§

All data are mean ± standard error; n = 5, respectively.
*; Significant differences were observed between SHRSP5/Dmcr rats fed SP and HFC diets for the same period, $p < 0.05$
†; Significant differences were observed between WKY/Izm rats fed SP and HFC diets for the same period, $p < 0.05$
‡; Significant different from SHRSP5/Dmcr rats fed the respective diet (the previous vs. following), $p < 0.05$
§; Significant different from SHRSP5/Dmcr and WKY/Izm rats fed the respective diet for 20 weeks, $p < 0.05$
AST; aspartate transaminase, ALT; alanine transaminase, ALB; albumin, A/G; albumin/globulin, T-Chol; total cholesterol, TG; triglyceride

compared between the different food–loading periods (4 weeks vs. 12 weeks and 12 weeks vs. 20 weeks). For the 20-week load, comparisons were made between SHRSP5/Dmcr and WKY/Izm rats. The biochemical data, NAS, and Ishak stage were compared between SHRSP5/Dmcr or WKY/Izm rat groups fed the different diets (SP or HFC) for the same duration, and between groups fed the same diet for different duration (4 weeks vs. 12 weeks and 12 weeks vs. 20 weeks). Comparisons were also made between the SHRSP5/Dmcr and WKY/Izm rats fed the same diet for 20 weeks. All statistical analyses were performed using the Mann-Whitney U-test, and statistical significance was set as $p < 0.05$.

3. Results

3.1. Physiological analysis

Changes in the body weight of rats in each group are shown in Fig. 1B. Both SHRSP5/Dmcr and WKY/Izm rats fed an HFC diet (H4, H12, H20, and H20W groups) had lower body weights than those in the SP groups (S4, S12, S20, and S20W groups). From 9–29 weeks of age, the HFC groups had significantly lower food intakes than the SP groups (Fig. 1C). Moreover, WKY/Izm and SHRSP5/Dmcr rats exhibited different limb muscle strength; WKY/Izm rats demonstrated stronger muscular strength from 9 to 29 weeks of age compared to SHRSP5/Dmcr rats. All groups showed increased muscle strength with age. Interestingly, starting at 16 weeks of age, SHRSP5/Dmcr rats fed an HFC diet exhibited a significantly slower increase in muscle strength compared to that of the SP groups; only the SHRSP5/Dmcr + HFC diet group showed decreased muscle strength at 28 weeks of age. In contrast, the WKY/Izm rats exhibited no difference in limb strength between the SP and HFC groups (Fig. 1D).

The electrically evoked muscle strength of the EDL, a fast muscle, increased with the increase in the feeding duration in the SP diet groups (S4 < S12 < S20). The S20W group was stronger muscle strength than the S20 group. In contrast, in the HFC groups, the H12 group showed a greater increase than the H4 group, and the H20 group showed a significant decrease in EDL strength compared to the H12 group. The muscle strength in the H20W group was remarkably stronger than the H20 group (Fig. 1E). The muscle strength of the SOL, a slow muscle, increased in both the SP and HFC groups (S4 < S12 < S20 group and H4 < H12 < H20 group). The SOL muscle strength was not significant between the S20 and S20W groups, and between the H20 (NASH) and H20W (NAFL) groups.

3.2. Biochemical analysis

The results of the biochemical analysis are shown in Table 1. AST, ALT, globulin, and T-Chol levels were significantly higher in the HFC groups in each loading period than in the SP groups. AST levels were markedly higher in the H20 group and similar in the H4, H12, and H20W groups. ALT levels were also highest in the H20 group, followed by the H12, H4, and H20W groups, but remained lower than AST levels. Globulin levels were highest in the H20 group, with levels almost two-higher than those found in the H4, H12, and H20W groups. T-Chol and TG were significantly higher in the H20 group, followed by the H20W, H12, and H4 groups. ALB levels were lower in the H4, H20W, H12, and H20 groups, in that order, but varied less between groups than the other parameters. The A/G ratio was lower in the HFC group than in the SP group, and the H20 group had the lowest level. Although there were some fluctuations in the biochemical data of the SP groups, the measurements were generally within normal ranges. AST levels were slightly higher in the S4 group than in the S12, S20, and S20W groups. ALT and TG levels were slightly lower in the S20W group than in the S4, S12, and S20 groups. ALB levels were slightly higher in the S20W group than in the S4, S12, and S20 groups. Globulin levels were slightly lower in the S4 group than in the S12, S20, and S20W groups. There were no differences in the A/G ratio between these groups. T-Chol levels were slightly higher in the S12 and S20 groups than in the S4 group and nearly two-fold higher in the S20W group than in the S12 and S20 groups.

3.3. Histopathological analysis of the liver

The tibial length was similar between the SP and HFC groups (Fig. 2A). Moreover, organ weights were calculated using the tibial length, which correlated with body height or growth degree (Fig. 2B-E). Liver weight/tibial length was significantly greater in the HFC groups than in the SP groups during each feeding period. Moreover, SHRSP5/Dmcr rats in the SP groups did not show any difference in liver weight/tibial length between the different feeding periods whereas those in the HFC groups showed a marked increase in the order of H4 < H12 < H20 groups. At 20 weeks of age, the liver weight in the H20W group was lower than that in the H20 group (Fig. 2B). Moreover, the spleen weight/tibial length was markedly increased in the H20 group compared to that in the S20 group. During the other feeding periods, a slightly increasing trend was observed in the HFC groups (Fig. 2C). Additionally, the EDL/tibial length tended to increase in the order S4 < S12 < S20. However, no increasing trend was observed in the HFC groups, and the EDL/tibial length was significantly lower in the H12 and H20 groups than that in the S12 and S20 groups. No significant differences were observed between the S20W and H20W groups (Fig. 2D). SOL/tibial length was similar to EDL/tibial length (Fig. 2E).

Histological analysis revealed that the livers of rats in the H4 group were whitish and enlarged compared to those of rats fed the SP diet. The whitish color of the liver was more pronounced in the H12 group than in the H4 group, and the livers of the H20 and H20W groups were brownish-yellow. In the H12 and H20 groups, the surface of the liver was uneven and hard whereas it was smooth in the

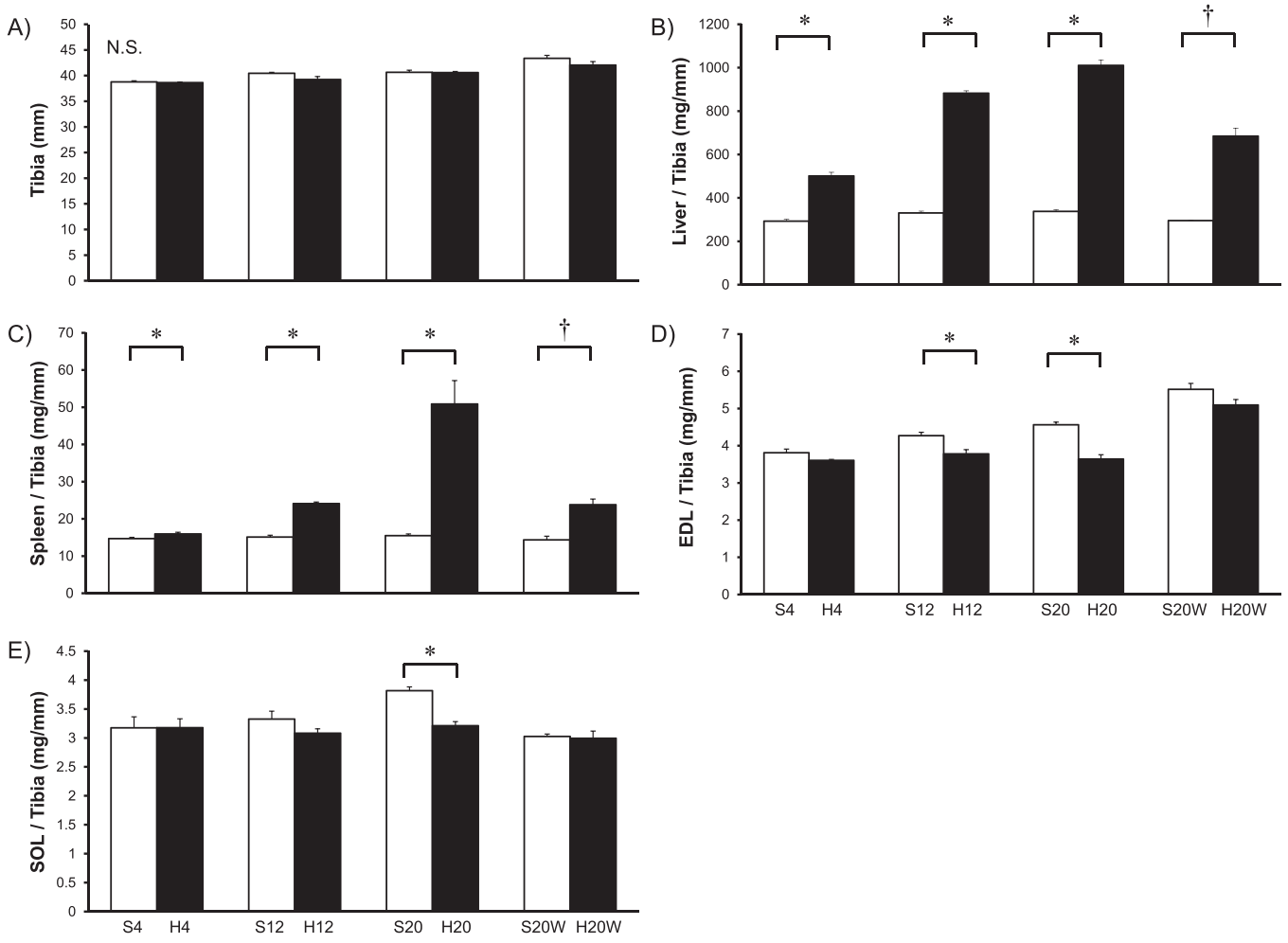

Fig. 2. The pathological analysis. The organ weight was corrected for tibial length. The tibial length was the same degree in all groups (A). The liver weight/tibial length was increased in order to the H4, H12, and H20 groups (B). The spleen weight/tibial length was markedly increased in the H20 group (C). The EDL and SOL weight/tibial length were significantly decreased in the H20 group (D, E). All data are mean ± standard error. * ; Significant differences were observed between SHRSP5/Dmcr rats fed SP and HFC diets for the same period, $p < 0.05$. †; Significant differences were observed between WKY/Izm rats fed SP and HFC diets for the same period, $p < 0.05$. SHRSP5/Dmcr: stroke-prone spontaneously hypertensive rat 5, SP: stroke-prone, HFC: high-fat and high-cholesterol diet, WKY: Wister Kyoto, EDL: extensor digitorum longus muscle, SOL: soleus muscle.

H20W group and SP groups. In contrast, no changes were observed in the livers of rats in the SP groups (Supplementary Fig. 3).

The livers of the SP groups did not exhibit lipid deposition, hepatocyte ballooning, and lymphocytic infiltration (Fig. 3A). However, ballooned hepatocytes as observed in the HFC groups (Fig. 3B, green arrow). Severe lipid droplets were observed in the H12 and H20 groups; however, they were considerably mild in the H4 and H20W groups (Fig. 3B, yellow arrow). In addition, lymphocytic infiltration was observed in the HFC groups and was the most severe in the H20 group (Fig. 3B, white arrow). Sight pericellular and/or perivascular fibrotic changes were observed in the livers of rats in the H4 group. The H12 group exhibited extensive areas of fibrosis and bridging structures between the portal-to-portal veins, with fibrosis extending from the portal-to-central veins. Furthermore, in the H20 group with a longer feeding period, the fibrotic area was enlarged and nodules were also observed. The livers of the H20W group exhibited pericellular and/or perivascular fibrotic changes, and some bridging structures between the portal-to-portal veins (Fig. 3B). In contrast, the livers of rats in the SP groups were normal (Fig. 3A).

NAS and fibrosis scores were calculated according to Kleiner et al., Elias et al., Ishak et al., and Goodman et al. (Table 2) (Elias et al., 2009; Goodman, 2007; Ishak et al., 1995; Kleiner et al., 2005). The mean steatosis grades in the H12 and H20 groups were 2.52 ± 0.08 and 2.48 ± 0.12, respectively, whereas the H20W group showed a low steatosis grade (0.60 ± 0.14). The SP and H4 groups scored 0 points. Moreover, although slight lobular inflammation was observed in the livers of the SP diet-fed rats, it was within normal limits. The rats in the HFC groups showed an increased number of inflammatory cells at 4 weeks of age (H4 group), which markedly increased at 20 weeks of age. Hepatocyte ballooning was not observed in the SP groups whereas it was observed in the same grade (2.00 points) in all HFC groups. NAS was increased with the duration of the HFC diet intake (H4: 3.84 ± 0.13, H12: 6.00 ± 0.28, H20: 7.32 ± 0.16). The H20W group had lower NAS levels (3.84 ± 0.30) than the H20 group, and the mean NAS was similar to that of the H4 group. The SP diet did not influence the Ishak stage (fibrosis grade) whereas the HFC diet significantly increased the Ishak stage in SHRSP5/Dmcr rats. The Ishak stage of WKY/Izm rats fed the HFC diet (H20W) was milder than that of rats in the H12 and H20 groups (H12: 3.40 ± 0.07, H20: 5.30 ± 0.19, H20W: 2.80 ± 0.26).

3.4. Histopathological findings of skeletal muscle

The muscle fiber cross-sections of both the EDL and SOL in the SP groups increased with the duration of the SP diet intake (S4 < S12 < S20 groups; Supplementary Fig. 4A, B). The SOL exhibited mild changes between the S20 and S20W groups whereas the EDL tended to be slightly larger in the S20W group. These results were similar to those of the electrically-induced muscle strength

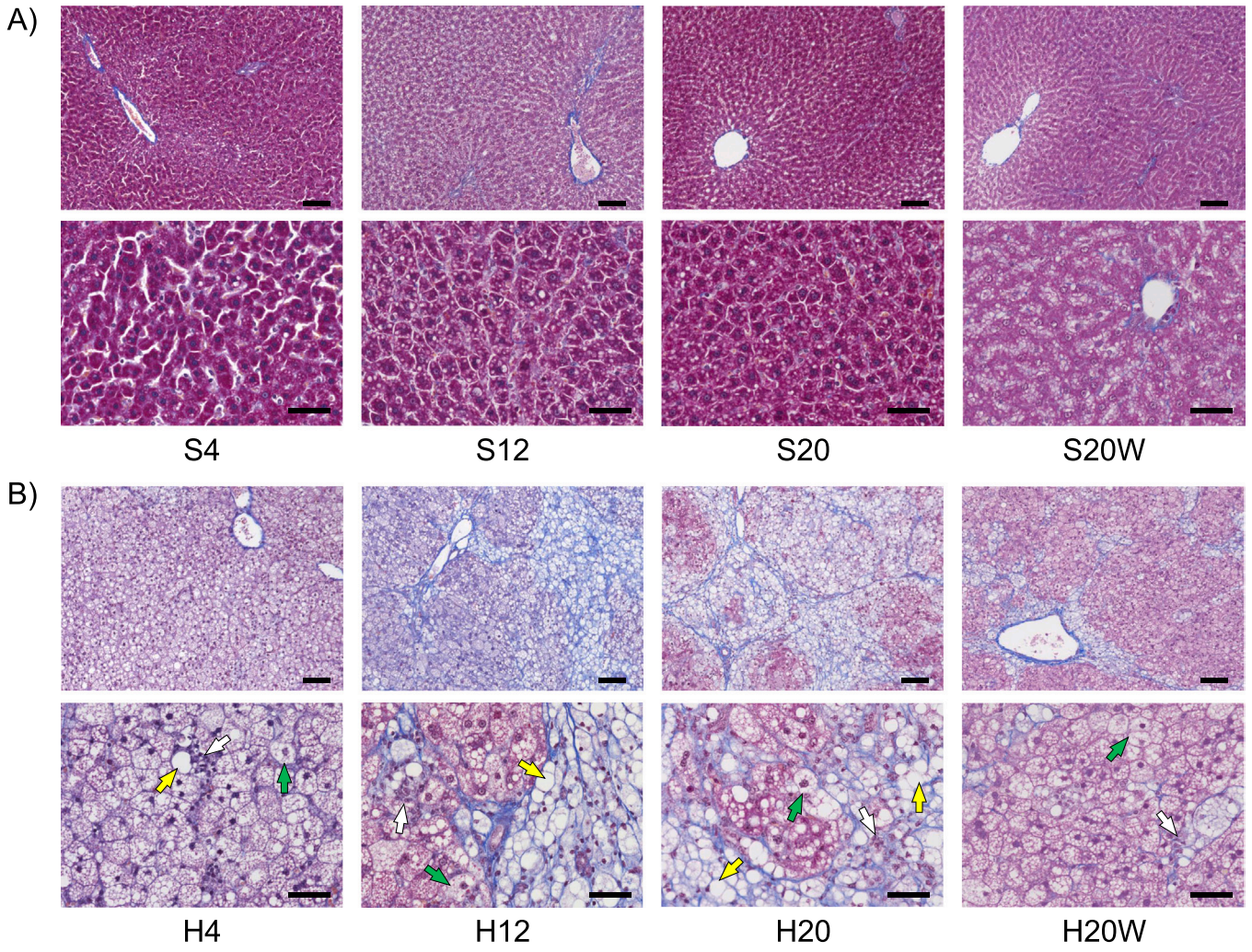

Fig. 3. Masson-trichrome staining of liver in SHRSP5/Dmcr and WKY/Izm rats fed an SP or HFC diet. The SP groups had no changes in liver lobule structure and hepatocytes (A). The HFC groups increased markedly ballooned hepatocytes (green arrow) and lobular inflammation (white arrow). In addition, the H12 and H20 groups noticeably increased lipid droplets (steatosis: yellow arrow) and fibrosis areas (blue staining area) (B). Scale bar = 100 μm (upper), 50 μm (lower). SHRSP5/Dmcr: stroke-prone spontaneously hypertensive rat 5, WKY: Wister Kyoto, SP: stroke-prone, HFC: high-fat and high-cholesterol diet.

experiments (Fig. 1E, F). Additionally, the EDL was larger in the H12 group than in the H4 group, and some fibers in the H20 group showed atrophy (Supplementary Fig. 4A). In contrast, the cross-section of the muscle fibers of the SOL of the HFC groups increased with the duration of the diet intake (H4 < H12 < H20 < H20W groups; Supplementary Fig. 4B). The SOL and EDL of the H20W group were slightly larger than those of the H20 group.

Fig. 4 showed the cross-sectional integral distribution of the fast muscle fibers, the major component fibers of the EDL, and slow muscle fibers, the major component fibers of the SOL, in the S20 and H20 groups. The number of small fast muscle fibers of the EDL increased (Fig. 4A) whereas the number of slow muscle fibers of the SOL muscle did not differ between the S20 and H20 groups (Fig. 4B).

Table 2
NAS and Ishak stage.

Groups	S4	S12	S20	S20W	H4	H12	H20	H20W
Steatosis grade	0	0	0	0	0	2.52 ± 0.08*‡	2.48 ± 0.12*	0.60 ± 0.14†§
Lobular inflammation	0.28 ± 0.14	0.28 ± 0.08	0.20 ± 0.06	0.52 ± 0.12§	1.84 ± 0.13*	1.48 ± 0.24*‡	2.84 ± 0.07*‡	1.24 ± 0.25†§
Hepatocyte ballooning	0	0	0	0	2.00 ± 0.00*	2.00 ± 0.00*	2.00 ± 0.00*	2.00 ± 0.00†
NAS	0.28 ± 0.14	0.28 ± 0.08	0.20 ± 0.06	0.52 ± 0.12§	3.84 ± 0.13*	6.00 ± 0.28*‡	7.32 ± 0.16*‡	3.84 ± 0.30†§
Ishak stage	0	0	0	0	0.90 ± 0.27*	3.40 ± 0.07*‡	5.30 ± 0.19*‡	2.80 ± 0.26†§

All data are mean ± standard error; n = 5, respectively.
*; Significant differences were observed between SHRSP5/Dmcr rats fed SP and HFC diets for the same period, $p < 0.05$
†; Significant differences were observed between WKY/Izm rats fed SP and HFC diets for the same period, $p < 0.05$
‡; Significant different from SHRSP5/Dmcr rats fed the respective diet (the previous vs. following), $p < 0.05$
§; Significant different from SHRSP5/Dmcr and WKY/Izm rats fed the respective diet for 20 weeks, $p < 0.05$
NAS; nonalcoholic fatty liver disease activity score

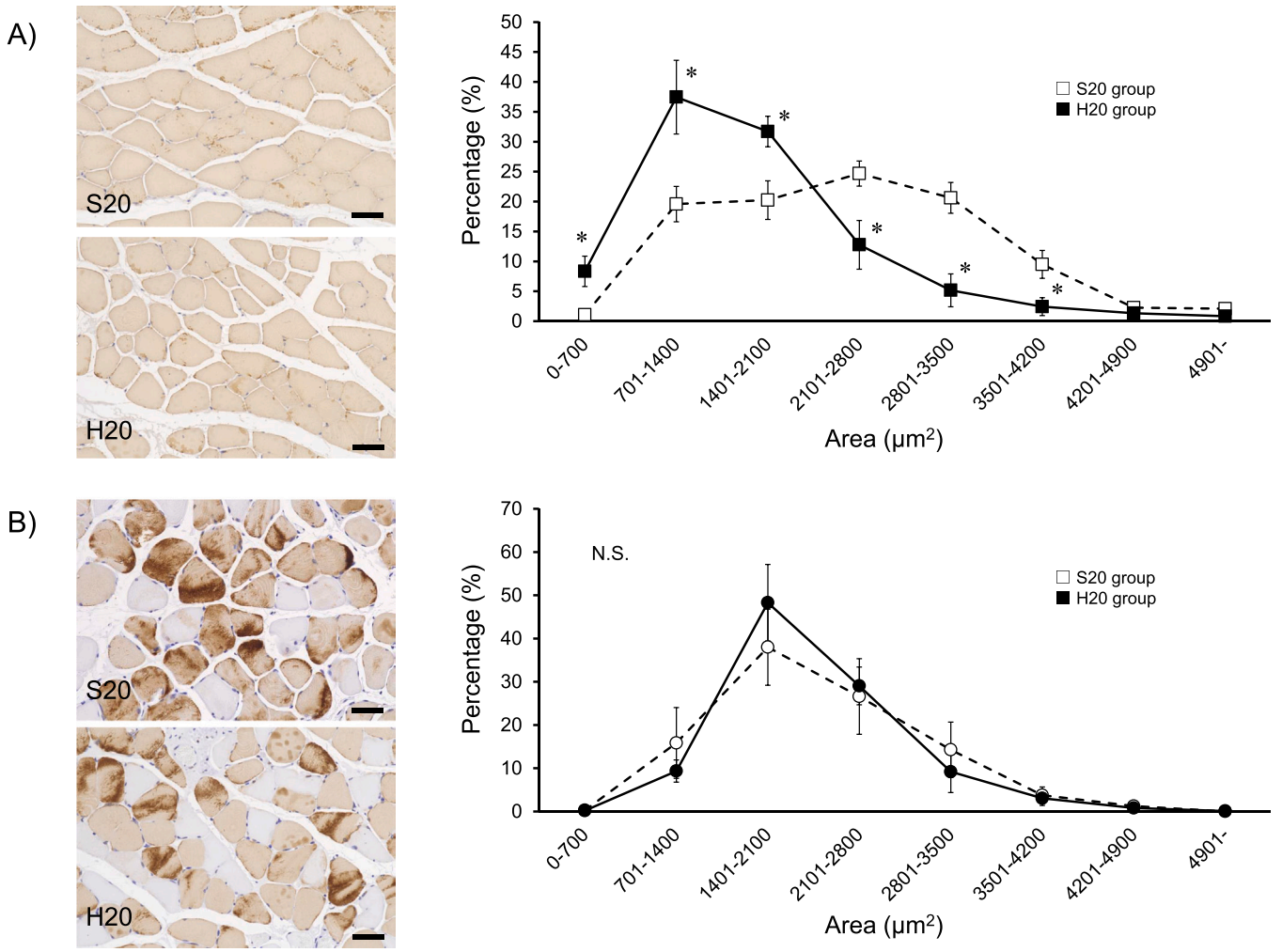

Fig. 4. Immunohistochemical staining and fiber fraction of fast and slow myofibers. The Fast muscle fibers distribution of the EDL (A) and slow muscle fibers distribution of the SOL (B) in the S20 and H20 groups. The EDL and SOL are mainly composed of fast and slow muscle fibers, respectively. The fast muscle fibers in the H20 group exhibited atrophy in the cross-sectional area of their constituent muscle fibers compared to the S20 group whereas no difference was observed in the slow muscle fibers. Scale bar = 100 μm. All data are mean ± standard error. *; Significant differences were observed between the S20 and H20 group, $p < 0.05$. EDL: extensor digitorum longus muscle, SOL: soleus muscle.

4. Discussion

4.1. Progression of NAFLD

In the present study, we demonstrated the progression of NAFLD/NASH in SHRSP5/Dmcr and WKY/Izm rats fed an SP/HFC diet and compared their biochemical and histopathological findings. SHRSP5/Dmcr rats, which are established from outbred WKY/Izm rats, were reported to develop NASH (severe fibrosis) and hyperlipidemia via an HFC diet (including 2% cholic acid) loading (Kitamori et al., 2012). Denk et al. noted that most models (except those with chemically or genetically induced porphyria or keratin 18-deficiency) did not exhibit ballooned hepatocytes and Mallory-Denk bodies, which are histological features of human NASH (Denk et al., 2019). However, SHRSP5/Dmcr rats fed an HFC diet developed ballooned hepatocytes due to high levels of hepatocyte injury, because they could not secrete water, protein, and small lipid droplets, and Mallory-Denk bodies associated with NASH progress (Kitamori et al., 2012; Naito et al., 2019). Thus, SHRSP5/Dmcr rats are suitable animal models for NASH, with histological similarities to human NASH pathology.

NAFLD or NASH is generally characterized by high total cholesterol levels in the serum (Fu et al., 2009; Puri et al., 2007). In our study, the T-Chol level of SHRSP5/Dmcr rats increased in the HFC groups compared to the SP groups in the order of the H4 < H12 < and H20 groups. The AST, ALT, globulin, and TG levels also showed a similar trend as T-Chol whereas the ALB and A/G ratios decreased with a longer dietary load (Table 1). The levels of AST and ALT, which are deviating enzymes, increase in patients with NAFLD/NASH as the disease progresses, with cirrhosis showing a predominance of AST. In this study, AST levels were considerably high compared to those of ALT in the H20 group; however, liver atrophy and morphological features of cirrhosis were not observed. Additionally, the level of ALB, one of the main serum proteins produced in the liver, is low in patients with liver injuries. In our study, low ALB levels were observed in rats as the HFC diet intake period increased. The A/G ratio, which represents the ratio of globulin to serum protein, was markedly lower in the H20 group than in normal rats fed the SP diet (Table 1). In other words, the H20 group was severely liver-damaged, suggesting that protein synthesis capacity was reduced. Serum TG levels also increased with the increase in the duration of the HFC diet, which is consistent with the report by Kitamori et al. (Kitamori et al., 2012). Although the HFC diet contains high cholesterol and lipids, non-obese and non-diabetic patients with NASH generally consume a high amount of dietary cholesterol and saturated fatty acid (Musso et al., 2003). In general, most patients with NAFLD/NASH show weight gain and insulin resistance; however, in our study, SHRSP5/Dmcr rats fed the HFC diet did not show an increase in body weight (Fig. 1B). In our previous study, we have

demonstrated that SHRSP5/Dmcr rats had normal glucose metabolism SHRSP5/Dmcr rats (oral glucose tolerance test, insulin tolerance test, and fasting serum glucose); in other words, SHRSP5/Dmcr rats have no insulin resistance (Watanabe et al., 2018). In the present study, the HFC diet contained 2% cholic acid. Watanabe M. et al. demonstrated that supplementation of high-fat obesogenic diets with cholic acid suppressed weight gain and insulin resistance in mice. This effect has been attributed to elevations in energy expenditure arising from thyroid hormone-mediated induction of brown adipose tissue thermogenesis (Watanabe et al., 2004; Watanabe et al., 2006). Excess cholic acid may have affected insulin resistance by promoting weight loss in the present study.

In the present study, the tibial length did not differ between the SP and HFC groups, suggesting that all groups exhibited similar growth during the food-loading periods (Fig. 2A). The liver weight/tibial length was significantly increased in the HFC groups, especially in the H20 group (Fig. 2B). Moreover, a NAS of 5.0 point or higher was defined as NASH, and the H12 and H20 groups were characterized as NASH in this experiment. We observed that hepatocyte ballooning scores were equal in all HFC groups; however, the steatosis grade was significantly increased after 12 weeks of diet intake, and lobular inflammation was approximately 1.4 points higher in the H20 group than in the H12 group (Table 2). Moreover, the Ishak stage, which evaluates fibrosis, also increased with the increase in the duration of the diet intake, and more nodules were observed in the H20 group (Table 2, Fig. 3B). Ishak et al. have defined a score of 5.0 points as incomplete cirrhosis and a score of 6.0 points as presumptive or definite cirrhosis; therefore, a 20-week HFC diet loading would lead to the development of a severe NASH state with advanced fibrosis, if not complete cirrhosis (Ishak et al., 1995). Kitamori et al. have evaluated fibrosis following the classification of Brunt et al. on a 5-stage scale (0–4), and they reported similar results to those in our study (Brunt et al., 1999; Kitamori et al., 2012). However, in the present study, rats in the H20W group had similar food intake to the H20 group until 27 weeks of age, and after 28 weeks of age, the intake of the HFC diet in the H20W group increased compared to that in the H20 group (Fig. 1C). Moreover, the degree of steatosis and fibrosis was milder in the H20W group than that of the H12 group; therefore, rats in the H20W group were characterized as NAFL rather than NASH (Table 2, Fig. 3B). Splenomegaly has been reported to be correlate with aggravated hepatic fibrosis in human NASH (Matsumoto et al., 2021). In the present study, the H20 group was morphologically enlarged and had significantly increased weights/tibial length (Fig. 2C, Supplementary Fig. 3). This result also supports that the hypothesis that the H20 group develops severe NASH.

4.2. Concomitant sarcopenia with the progression of NASH

Sarcopenia is defined by the Asian Working Group for Sarcopenia 2019 as a disease characterized by a decrease in skeletal muscle mass and loss of muscle strength and/or physical function (Chen et al., 2020). However, “concomitant diseases” were not mentioned and were described only as age-related. Disease-induced sarcopenia was not mentioned because its mechanism and other factors are complex and vary depending on the disease. Sarcopenia has been reported to be associated with cachexia, diabetes, and chronic kidney disease (Liccini and Malmstrom, 2016; Meza-Valderrama et al., 2021; Sabatino et al., 2021). In Japan, the Japan Society of Hepatology has developed its criteria for determining sarcopenia associated with chronic liver disease; thus, secondary sarcopenia is an important disease concept (Nishikawa et al., 2016). NAFLD/NASH is reported that associated with sarcopenia, which is characterized by reduced muscle tissue (Hong et al., 2014; Issa et al., 2014). Lee et al. have shown using the Korea National Health and Nutrition Examination Survey (KNHANES 2008–2011) that sarcopenia is significantly associated with hepatic fibrosis in NAFLD, independent of obesity and insulin resistance (Lee et al., 2015). Petta et al. reported that sarcopenia was associated with severe fibrosis and steatosis in Western patients with NAFLD (Petta et al., 2017). However, the causal association between these 2 diseases remains unknown; therefore, the accumulation of knowledge from clinical and epidemiological studies and basic research is essential to understand this causal association. In this study, we examined whether the SHRSP5/Dmcr rat, a NASH model rat, would be a useful animal model of secondary sarcopenia for basic research.

Skeletal muscles are composed of type I (slow twitch) and type II (fast twitch) myofibers. Sarcopenia results in a decrease in the size and number of muscle fibers, especially type II fibers, with significant atrophy (Lexell et al., 1988). Furthermore, a type-transition from type II fibers to type I fibers occurs in sarcopenia (Ciciliot et al., 2013; Verdijk et al., 2014). In this study, muscle weight was significantly reduced in the H12 and H20 groups for both fast (EDL) and slow muscles (SOL) compared to the S12 and S20 groups (Fig. 2D, E). Limb muscle strength remained significantly lower with the progression of NAFLD/NASH only in SHRSP5/Dmcr rats fed the HFC diet, and began to decrease at 28 weeks of age (Fig. 1D). In addition, the analysis of electrically evoked-muscle strength in the EDL (fast muscle) and SOL (slow muscle) revealed that the strength of the SOL increased with growth whereas that of the EDL decreased in the H20 group (Fig. 1E, F). In the pathological analysis, many fibers with small cross-sections were observed only in the EDLs of the H20 group by HE staining (Supplementary Figs. 4A). Moreover, IHC staining of the cross-section of EDL (fast-) and SOL (slow-) twitch fibers in the S20 and H20 groups revealed that the cross-sectional area was reduced only in the EDL of the H20 group (Fig. 4A, B). However, we could not determine whether the transition from type II to type I fibers occurred. Muscle atrophy includes disuse muscle atrophy caused by reduced activity, which must be carefully differentiated from sarcopenia. Disuse muscle atrophy is generally characterized by significant atrophy of slow twitch fibers and a transition from type I to type II fibers (Burnham et al., 1997; Gallagher et al., 2005; Grimby et al., 1976). In this study, IHC staining of fast and slow twitch fibers showed a difference in fiber thickness (cross-sectional area) between the SP and HFC groups. However, skeletal muscle atrophy was not observed in the SOL; thus, disuse muscle atrophy did not develop (Fig. 4B). Therefore, these results suggest that the H20 group satisfied the “loss of skeletal muscle mass” and “loss of muscle strength” criteria as defined by the Asian Working Group for Sarcopenia 2019, and developed sarcopenia. In general, when the liver is damaged and gluconeogenesis is reduced, the organism compensates for amino acids (branched-chain amino acids) derived from the dissolution of skeletal muscle, which is associated with sarcopenia in NAFLD/NASH. In the present study, in the H20 group, biochemical (AST, ALT, ALB, and A/G ratio) and histopathological analyses (Masson-trichrome staining, NAS, and Ishak stage) indicated that the liver was severely damaged. Therefore, the compensatory dissolution of skeletal muscle, especially fast muscle, in the H20 group may play a role in the development of sarcopenia.

4.3. Limitations

Many patients with NASH also have obesity and insulin resistance, and insulin resistance can significantly affect skeletal muscle function. Since SHRSP5/Dmcr rats did not exhibit obesity and insulin resistance, this model should be used carefully depending on the purpose. Sarcopenia also accompanies NASH in some lean patients, and insulin resistance and obesity have been reported to be independently associated with sarcopenia and poor prognosis of NAFLD/NASH. Therefore, SHRSP5/Dmcr rats which lack obesity and insulin resistance may be useful in investigating the relationships between NASH and sarcopenia.

Recently, bile acids, particularly cholic acid and deoxycholic acid, have been reported to be involved in skeletal muscle atrophy (Abrigo et al., 2021). The HFC diet contained cholic acid, and its effect was confirmed in the H20W group; however, no pathological features of sarcopenia were observed. Serum bile acids are increased in patients with NAFLD/NASH (Ferslew et al., 2015; Jiao et al., 2018). In this rat model, we demonstrated that bile acid levels were increased and the bile acid profile was altered, aggravating NAFLD/NASH pathology (Yamamoto et al., 2020). We were unable to investigate whether bile acids are involved in the concomitant development of NAFLD/NASH and sarcopenia. However, in the present study, at least cholic acid in the HFC diet has no effect on the development of sarcopenia. We need further investigation into the molecular mechanisms linking NASH/liver fibrosis to sarcopenia.

5. Conclusion

We demonstrated that SHRSP5/Dmcr rats, an animal model of NASH, developed disease-induced sarcopenia as NASH progressed. This model, without insulin resistance and obesity, may be useful for investigating the mechanism and prevention and/or amelioration method for sarcopenia.

Funding

This work was supported by JSPS KAKENHI (Grants-in-Aid for Scientific Research), Grant-in-Aid for JSPS Fellows Grant Number JP21J23123, and The Association for Fordays Self-Reliance Support in Japan to S. Yamamoto.

Ethical Statement

All experimental procedures on animals were in strict accordance with the recommendations of the standards of Care and Management of Laboratory Animals and Relief of Pain published by the Japanese Ministry of Environment (2006) and were approved by the Animal Experiment Committee of Okayama University (approval No. OKU-2021208).

CRediT authorship contribution statement

Shusei Yamamoto: Conceptualization, Funding acquisition, Project administration, Data curation, Formal analysis, Investigation, Visualization, Writing-original draft. **Koki Honma**: Data curation, Investigation. **Moe Fujii**: Data curation, Investigation. **Mai Kakimoto**: Data curation, Investigation. **Sora Kirihara**: Data curation, Investigation. **Hinako Nakayama**: Data curation, Investigation. **Kazuya Kitamori**: Investigation, Writing-review & editing. **Ikumi Sato**: Investigation. **Satoshi Hirohata**: Supervision, Writing-review & editing. **Shogo Watanabe**: Project administration, Supervision, Writing-review & editing.

Declaration of Competing Interest

The authors declare that they have no known competing financial interests or personal relationships that could have appeared to influence the work reported in this paper.

Acknowledgement

The authors thank Mr. Eito Matsumoto, Ms. Sana Matsushita, Ms. Tomona Kaihara, Ms. Minami Shimada, Ms. Nao Kuwada, Ms. Saho Suto, Ms. Suzu Ito, and Mr. Taketo Fukuoka for technical assistance during the physiological analysis. We also thank Okayama University Medical School for their technical assistance in the histopathological analysis, and Editage (www.editage.com) for English language editing.

Appendix A. Supporting information

Supplementary data associated with this article can be found in the online version at doi:10.1016/j.aanat.2023.152104.

References

Abrigo, J., Gonzalez, F., Aguirre, F., Tacchi, F., Gonzalez, A., Meza, M.P., Simon, F., Cabrera, D., Arrese, M., Karpen, S., Cabello-Verrugio, C., 2021. Cholic acid and deoxycholic acid induce skeletal muscle atrophy through a mechanism dependent on TGR5 receptor. J. Cell. Physiol. 236, 260–272.

Brunt, E.M., Janney, C.G., Di Bisceglie, A.M., Neuschwander-Tetri, B.A., Bacon, B.R., 1999. Nonalcoholic steatohepatitis: a proposal for grading and staging the histological lesions. Am. J. Gastroenterol. 94, 2467–2474.

Burnham, R., Martin, T., Stein, R., Bell, G., MacLean, I., Steadward, R., 1997. Skeletal muscle fibre type transformation following spinal cord injury. Spinal Cord. 35, 86–91.

Cabrera, D., Ruiz, A., Cabello-Verrugio, C., Brandan, E., Estrada, L., Pizarro, M., Solis, N., Torres, J., Barrera, F., Arrese, M., 2016. Diet-Induced nonalcoholic fatty liver disease is associated with sarcopenia and decreased serum insulin-like growth factor-1. Dig. Dis. Sci. 61, 3190–3198.

Chen, L.K., Woo, J., Assantachai, P., Auyeung, T.W., Chou, M.Y., Iijima, K., Jang, H.C., Kang, L., Kim, M., Kim, S., Kojima, T., Kuzuya, M., Lee, J.S.W., Lee, S.Y., Lee, W.J., Lee, Y., Liang, C.K., Lim, J.Y., Lim, W.S., Peng, L.N., Sugimoto, K., Tanaka, T., Won, C.W., Yamada, M., Zhang, T., Akishita, M., Arai, H., 2020. Asian working group for sarcopenia: 2019 consensus update on sarcopenia diagnosis and treatment. J. Am. Med. Dir. Assoc. 21, 300–307 e302.

Ciciliot, S., Rossi, A.C., Dyar, K.A., Blaauw, B., Schiaffino, S., 2013. Muscle type and fiber type specificity in muscle wasting. Int. J. Biochem. Cell Biol. 45, 2191–2199.

Cruz-Jentoft, A.J., Sayer, A.A., 2019. Sarcopenia. Lancet 393, 2636–2646.

Denk, H., Abuja, P.M., Zatloukal, K., 2019. Animal models of NAFLD from the pathologist's point of view. Biochim. Biophys. Acta Mol. Basis. Dis. 1865, 929–942.

Elias Jr., J., Altun, E., Zacks, S., Armao, D.M., Woosley, J.T., Semelka, R.C., 2009. MRI findings in nonalcoholic steatohepatitis: correlation with histopathology and clinical staging. Magn. Reson. Imaging 27, 976–987.

Ferslew, B.C., Xie, G., Johnston, C.K., Su, M., Stewart, P.W., Jia, W., Brouwer, K.L., Barritt, A.St, 2015. Altered bile acid metabolome in patients with nonalcoholic steatohepatitis. Dig. Dis. Sci. 60, 3318–3328.

Fu, C.C., Chen, M.C., Li, Y.M., Liu, T.T., Wang, L.Y., 2009. The risk factors for ultrasound-diagnosed non-alcoholic fatty liver disease among adolescents. Ann. Acad. Med. Singap. 38, 15–17.

Gallagher, P., Trappe, S., Harber, M., Creer, A., Mazzetti, S., Trappe, T., Alkner, B., Tesch, P., 2005. Effects of 84-days of bedrest and resistance training on single muscle fibre myosin heavy chain distribution in human vastus lateralis and soleus muscles. Acta Physiol. Scand. 185, 61–69.

Goodman, Z.D., 2007. Grading and staging systems for inflammation and fibrosis in chronic liver diseases. J. Hepatol. 47, 598–607.

Grimby, G., Broberg, C., Krotkiewska, I., Krotkiewski, M., 1976. Muscle fiber composition in patients with traumatic cord lesion. Scand. J. Rehabil. Med. 8, 37–42.

Habig, G., Smaltz, C., Halegoua-DeMarzio, D., 2021. Presence and Implications of Sarcopenia in non-alcoholic Steatohepatitis. Metabolites 11, 242.

Hiraoka, A., Michitaka, K., Kiguchi, D., Izumoto, H., Ueki, H., Kaneto, M., Kitahata, S., Aibiki, T., Okudaira, T., Tomida, H., Miyamoto, Y., Yamago, H., Suga, Y., Iwasaki, R., Mori, K., Miyata, H., Tsubouchi, E., Kishida, M., Ninomiya, T., Kohgami, S., Hirooka, M., Tokumoto, Y., Abe, M., Matsuura, B., Hiasa, Y., 2017. Efficacy of branched-chain amino acid supplementation and walking exercise for preventing sarcopenia in patients with liver cirrhosis. Eur. J. Gastroenterol. Hepatol. 29, 1416–1423.

Hong, H.C., Hwang, S.Y., Choi, H.Y., Yoo, H.J., Seo, J.A., Kim, S.G., Kim, N.H., Baik, S.H., Choi, D.S., Choi, K.M., 2014. Relationship between sarcopenia and nonalcoholic fatty liver disease: the Korean Sarcopenic Obesity Study. Hepatology 59, 1772–1778.

Ishak, K., Baptista, A., Bianchi, L., Callea, F., De Groote, J., Gudat, F., Denk, H., Desmet, V., Korb, G., MacSween, R.N., et al., 1995. Histological grading and staging of chronic hepatitis. J. Hepatol. 22, 696–699.

Issa, D., Alkhouri, N., Tsien, C., Shah, S., Lopez, R., McCullough, A., Dasarathy, S., 2014. Presence of sarcopenia (muscle wasting) in patients with nonalcoholic steatohepatitis. Hepatology 60, 428–429.

Jiao, N., Baker, S.S., Chapa-Rodriguez, A., Liu, W., Nugent, C.A., Tsompana, M., Mastrandrea, L., Buck, M.J., Baker, R.D., Genco, R.J., Zhu, R., Zhu, L., 2018. Suppressed hepatic bile acid signalling despite elevated production of primary and secondary bile acids in NAFLD. Gut 67, 1881–1891.

Kitamori, K., Naito, H., Tamada, H., Kobayashi, M., Miyazawa, D., Yasui, Y., Sonoda, K., Tsuchikura, S., Yasui, N., Ikeda, K., Moriya, T., Yamori, Y., Nakajima, T., 2012. Development of novel rat model for high-fat and high-cholesterol diet-induced steatohepatitis and severe fibrosis progression in SHRSP5/Dmcr. Environ. Health Prev. Med. 17, 173–182.

Kleiner, D.E., Brunt, E.M., Van Natta, M., Behling, C., Contos, M.J., Cummings, O.W., Ferrell, L.D., Liu, Y.C., Torbenson, M.S., Unalp-Arida, A., Yeh, M., McCullough, A.J., Sanyal, A.J., 2005. Design and validation of a histological scoring system for nonalcoholic fatty liver disease. Hepatology 41, 1313–1321.

Koo, B.K., Kim, D., Joo, S.K., Kim, J.H., Chang, M.S., Kim, B.G., Lee, K.L., Kim, W., 2017. Sarcopenia is an independent risk factor for non-alcoholic steatohepatitis and significant fibrosis. J. Hepatol. 66, 123–131.
Kozaki, Y., Umetsu, R., Mizukami, Y., Yamamura, A., Kitamori, K., Tsuchikura, S., Ikeda, K., Yamori, Y., 2015. Peripheral gene expression profile of mechanical hyperalgesia induced by repeated cold stress in SHRSP5/Dmcr rats. J. Physiol. Sci. 65, 417–425.
Lee, Y.H., Jung, K.S., Kim, S.U., Yoon, H.J., Yun, Y.J., Lee, B.W., Kang, E.S., Han, K.H., Lee, H.C., Cha, B.S., 2015. Sarcopaenia is associated with NAFLD independently of obesity and insulin resistance: nationwide surveys (KNHANES 2008-2011). J. Hepatol. 63, 486–493.
Lexell, J., Taylor, C.C., Sjöström, M., 1988. What is the cause of the ageing atrophy? total number, size and proportion of different fiber types studied in whole vastus lateralis muscle from 15- to 83-year-old men. J. Neurol. Sci. 84, 275–294.
Liccini, A., Malmstrom, T.K., 2016. Frailty and sarcopenia as predictors of adverse health outcomes in persons with diabetes mellitus. J. Am. Med. Dir. Assoc. 17, 846–851.
Matsumoto, N., Kumagawa, M., Ogawa, M., Kaneko, M., Watanabe, Y., Nakagawara, H., Masuzaki, R., Kanda, T., Moriyama, M., Sugitani, M., 2021. Ultrasonographic grayscale findings related to fibrosis in patients with non-alcoholic fatty liver disease: comparison with transient elastography and Fib-4. Index. J. Med. Ultrason 48, 323–333 (2001).
Meza-Valderrama, D., Marco, E., Dávalos-Yerovi, V., Muns, M.D., Tejero-Sánchez, M., Duarte, E., Sánchez-Rodríguez, D., 2021. Sarcopenia malnutrition and cachexia: adapting definitions and terminology of nutritional disorders in older people with cancer. Nutrients 13, 761.
Mohta, S., Anand, A., Sharma, S., Qamar, S., Agarwal, S., Gunjan, D., Singh, N., Madhusudhan, K.S., Pandey, R.M., Saraya, A., 2022. Randomised clinical trial: effect of adding branched chain amino acids to exercise and standard-of-care on muscle mass in cirrhotic patients with sarcopenia. Hepatol. Int. 16, 680–690.
Musso, G., Gambino, R., De Michieli, F., Cassader, M., Rizzetto, M., Durazzo, M., Fagà, E., Silli, B., Pagano, G., 2003. Dietary habits and their relations to insulin resistance and postprandial lipemia in nonalcoholic steatohepatitis. Hepatology 37, 909–916.
Nachit, M., De Rudder, M., Thissen, J.P., Schakman, O., Bouzin, C., Horsmans, Y., Vande Velde, G., Leclercq, I.A., 2021. Myosteatosis rather than sarcopenia associates with non-alcoholic steatohepatitis in non-alcoholic fatty liver disease preclinical models. J. Cachex. Sarcopenia Muscle 12, 144–158.
Naito, H., Yoshikawa-Bando, Y., Yuan, Y., Hashimoto, S., Kitamori, K., Yatsuya, H., Nakajima, T., 2019. High-fat and high-cholesterol diet decreases phosphorylated inositol-requiring kinase-1 and inhibits autophagy process in rat liver. Sci. Rep. 9, 12514.
Nd, A.M., 2019. Non-alcoholic fatty liver disease, an overview. Integr. Med. 18, 42–49.
Nishikawa, H., Shiraki, M., Hiramatsu, A., Moriya, K., Hino, K., Nishiguchi, S., 2016. Japan society of hepatology guidelines for sarcopenia in liver disease Recommendation from the working group for creation of sarcopenia assessment criteria (1st edition). Hepatol. Res. 46, 951–963.
Petta, S., Ciminnisi, S., Di Marco, V., Cabibi, D., Cammà, C., Licata, A., Marchesini, G., Craxì, A., 2017. Sarcopenia is associated with severe liver fibrosis in patients with non-alcoholic fatty liver disease. Aliment. Pharmacol. Ther. 45, 510–518.
Puri, P., Baillie, R.A., Wiest, M.M., Mirshahi, F., Choudhury, J., Cheung, O., Sargeant, C., Contos, M.J., Sanyal, A.J., 2007. A lipidomic analysis of nonalcoholic fatty liver disease. Hepatology 46, 1081–1090.
Rinella, M.E., 2015. Nonalcoholic fatty liver disease: a systematic review. JAMA 313, 2263–2273.
Sabatino, A., Cuppari, L., Stenvinkel, P., Lindholm, B., Avesani, C.M., 2021. Sarcopenia in chronic kidney disease: what have we learned so far. J. Nephrol. 34, 1347–1372.
Schindelin, J., Arganda-Carreras, I., Frise, E., Kaynig, V., Longair, M., Pietzsch, T., Preibisch, S., Rueden, C., Saalfeld, S., Schmid, B., Tinevez, J.Y., White, D.J., Hartenstein, V., Eliceiri, K., Tomancak, P., Cardona, A., 2012. Fiji: an open-source platform for biological-image analysis. Nat. Methods 9, 676–682.
Sweet, J.G., Chan, S.L., Cipolla, M.J., 2015. Effect of hypertension and carotid occlusion on brain parenchymal arteriole structure and reactivity. J. Appl. Physiol. 119, 817–823.
Verdijk, L.B., Snijders, T., Drost, M., Delhaas, T., Kadi, F., van Loon, L.J., 2014. Satellite cells in human skeletal muscle; from birth to old age. Age 36, 545–547.
Watanabe, M., Houten, S.M., Wang, L., Moschetta, A., Mangelsdorf, D.J., Heyman, R.A., Moore, D.D., Auwerx, J., 2004. Bile acids lower triglyceride levels via a pathway involving FXR, SHP, and SREBP-1c. J. Clin. Investig. 113, 1408–1418.
Watanabe, M., Houten, S.M., Mataki, C., Christoffolete, M.A., Kim, B.W., Sato, H., Messaddeq, N., Harney, J.W., Ezaki, O., Kodama, T., Schoonjans, K., Bianco, A.C., Auwerx, J., 2006. Bile acids induce energy expenditure by promoting intracellular thyroid hormone activation. Nature 439, 484–489.
Watanabe, S., Kumazaki, S., Kusunoki, K., Inoue, T., Maeda, Y., Usui, S., Shinohata, R., Ohtsuki, T., Hirohata, S., Kusachi, S., Kitamori, K., Mori, M., Yamori, Y., Oka, H., 2018. A high-fat and high-cholesterol diet induces cardiac fibrosis, vascular endothelial, and left ventricular diastolic dysfunction in SHRSP5/Dmcr Rats. J. Atheroscler. Thromb. 25, 439–453.
Yamamoto, S., Sato, I., Fukuhama, N., Akiyama, N., Sakai, M., Kumazaki, S., Ran, S., Hirohata, S., Kitamori, K., Yamori, Y., Watanabe, S., 2020. Bile acids aggravate nonalcoholic steatohepatitis and cardiovascular disease in SHRSP5/Dmcr rat model. Exp. Mol. Pathol. 114, 104437.
Younes, R., Bugianesi, E., 2019. NASH in Lean Individuals. Semin. Liver Dis. 39, 86–95.
Younossi, Z.M., Koenig, A.B., Abdelatif, D., Fazel, Y., Henry, L., Wymer, M., 2016. Global epidemiology of nonalcoholic fatty liver disease-Meta-analytic assessment of prevalence incidence and outcomes. Hepatology 64, 73–84.
Yu, R., Shi, Q., Liu, L., Chen, L., 2018. Relationship of sarcopenia with steatohepatitis and advanced liver fibrosis in non-alcoholic fatty liver disease: a meta-analysis. BMC Gastroenterol. 18, 51.